Speciation of Antimony in PET Bottles Produced in Japan and China by X-ray Absorption Fine Structure Spectroscopy

ARTICLE *in* ENVIRONMENTAL SCIENCE AND TECHNOLOGY · JANUARY 2009

Impact Factor: 5.33 · DOI: 10.1021/es802073x · Source: PubMed

5 AUTHORS, INCLUDING:

Takaaki Itai
CNRS-GET
43 PUBLICATIONS **341** CITATIONS
SEE PROFILE

Guodong Zheng
Chinese Academy of Sciences
77 PUBLICATIONS **617** CITATIONS
SEE PROFILE

Article

Speciation of Antimony in PET Bottles Produced in Japan and China by X-ray Absorption Fine Structure Spectroscopy

Yoshio Takahashi, Kyoko Sakuma, Takaaki Itai, Guodong Zheng, and Satoshi Mitsunobu

Environ. Sci. Technol., **2008**, 42 (24), 9045-9050 • Publication Date (Web): 14 November 2008

Speciation of Antimony in PET Bottles Produced in Japan and China by X-ray Absorption Fine Structure Spectroscopy

YOSHIO TAKAHASHI,*,† KYOKO SAKUMA,† TAKAAKI ITAI,† GUODONG ZHENG,‡ AND SATOSHI MITSUNOBU†

Department of Earth and Planetary Systems Science, Hiroshima University Hiroshima 739-8526, Japan; Institute of Geology and Geophysics, Chinese Academy of Sciences, Lanzhou 730000, P.R. China.

Received July 25, 2008. Revised manuscript received October 5, 2008. Accepted October 16, 2008.

The oxidation state and coordination environment of antimony (Sb) incorporated into polyethylene terephthalate (PET) bottles were estimated based on X-ray absorption fine structure (XAFS) at Sb K-edge. Prior to XAFS analyses, Sb concentrations in 177 PET bottles collected in Japan and China were determined, showing that 30.5% and 100% of Japanese and Chinese PET bottles, respectively, contained more than 10 mg/kg of Sb. Most of the bottles used for aseptic cold filling and carbonated drinks contained a larger amount of Sb. Extended X-ray absorption fine structure (EXAFS) showed that the first neighboring atom of Sb in PET was estimated to be oxygen with a coordination number of about three. In addition, the contribution of Sb to Sb shell was discounted in the EXAFS, showing that Sb was not present as Sb_2O_3 in PET, although Sb was initially added as Sb_2O_3 in the production of PET. This information is consistent with the coordination environment estimated from the polycondensation reaction catalyzed by Sb, where Sb can be present as either Sb glycolate or Sb glycolate binding to the end group of the PET polymer. X-ray absorption near-edge structure (XANES) showed that Sb(III) initially added as Sb_2O_3 into PET was partially oxidized and the Sb(V) fractions reached approximately 50% in some samples. However, the oxidation state and coordination environment of Sb in PET had no relationship with the concentrations of Sb that leached into water from PET. Based on the present XAFS results and previous studies on the effects of temperature and others, it was concluded that the leaching behavior of Sb into water is primarily due to the degradation of PET itself, but is not related to the Sb species in the PET bottles.

1. Introduction

Antimony (Sb) has been frequently used as a catalyst of polycondensation reaction to produce polyethylene terephthalate (PET) (*1, 2*). As a result, Sb is incorporated into some PET bottles used for beverages at a concentration level of 100−300 mg/kg (*1, 2*). Considering its high toxicity (*3*−*10*), the possible leaching of Sb into beverages is of great concern, which has motivated various studies on Sb content in PET bottles and leaching into beverages (*3*−*7*). In these studies, effects of pH, water temperature, elapsed time, and others on the concentration of Sb leaching have been examined. In addition, the influence of beverage type in PET bottles has been studied, especially in terms of the complexation effect of Sb with ligands in the liquid (such as citrus juice or acetic acid) that may cause Sb leaching to a greater degree (*5*−*7*). However, there have been no studies dealing with the direct characterization of Sb species in PET so far, such as the oxidation state and local structural environment around Sb, which can be related to its leaching into the liquid, as seen from the Sb behavior in natural environment (*8*−*11*). Since Sb is initially added as Sb_2O_3 in the production of PET (*1*), possible oxidation of Sb(III) should be verified considering that the leaching behavior of Sb may depend on its oxidation state.

There is relatively scarce knowledge on the chemical state of Sb in PET, so X-ray absorption fine structure (XAFS) was employed to obtain its atomic scale information. XAFS spectroscopy consisting of X-ray absorption near-edge structure (XANES) and extended X-ray absorption fine structure (EXAFS) was employed, which gives independent information such as the oxidation state and local structure of Sb (= coordination number and bond lengths to neighboring atoms), respectively. Although XAFS has been employed in various environmental studies (*8, 11*−*15*), its application to the speciation of Sb in PET has not yet been reported. Prior to the XAFS analyses, Sb concentrations in PET bottles have been determined in 105 and 72 brands of bottles sold in Japan and China, respectively. A relatively high content of Sb (170−220 mg/kg) has been reported for PET bottles in Japan (*5*) but not documented for those in China. Subsequently, these PET bottles have been used for XAFS measurement. In addition, leaching experiments have been done to investigate the possible relationship between the difference in the chemical state of Sb in PET and its leachability in water.

2. Experimental Section

2.1. PET Bottles and Reference Materials. Commercially available PET bottles composed of 105 brands (from 25 manufacturing corporations) were collected in Hiroshima (Japan) in April 2007, whereas Chinese PET bottles of 72 brands (from 32 corporations) were collected in Shanghai (China) in November 2007. Previous studies by Shotyk and his co-workers examined PET containers for natural waters (*3, 4*). In this study, PET bottles containing any beverages such as water, juice, tea, coffee, and carbonate beverages were used because the type of PET bottle is different depending on its contents, as will be described later. The Japanese PET bottles were transparent, while some Chinese bottles were colored in blue or green. The thickness of each PET bottle was examined by a micrometer caliper, and its thickness ranged from 10 to 45 μm. Senarmontite (Sb_2O_3; structure was confirmed by powder X-ray diffraction), Sb_2O_5, $KSb(OH)_6$, and $Sb(OH)_6^-$ solution prepared from dissolution of $KSb(OH)_6$ in water were used as reference materials of the Sb species. All the reagents at analytical grade were obtained from Aldrich Co. Ltd.

2.2. Determination of Sb Concentrations in PET. Microwave digestion using acids has often been used to decompose PET in previous studies (*5, 6*). Hence, this method was also employed using a mixture of conc. HNO_3 (0.5 mL) and 30 wt% H_2O_2 (1.5 mL) in PTFE digestion vessels for every 60 mg of PET. However, white residual materials were found

* Corresponding author phone: +81-82-424-7460; fax: +81-82-424-0735; e-mail: ytakaha@hiroshima-u.ac.jp.
† Hiroshima University.
‡ Institute of Geology and Geophysics.

10.1021/es802073x CCC: $40.75
Published on Web 11/14/2008

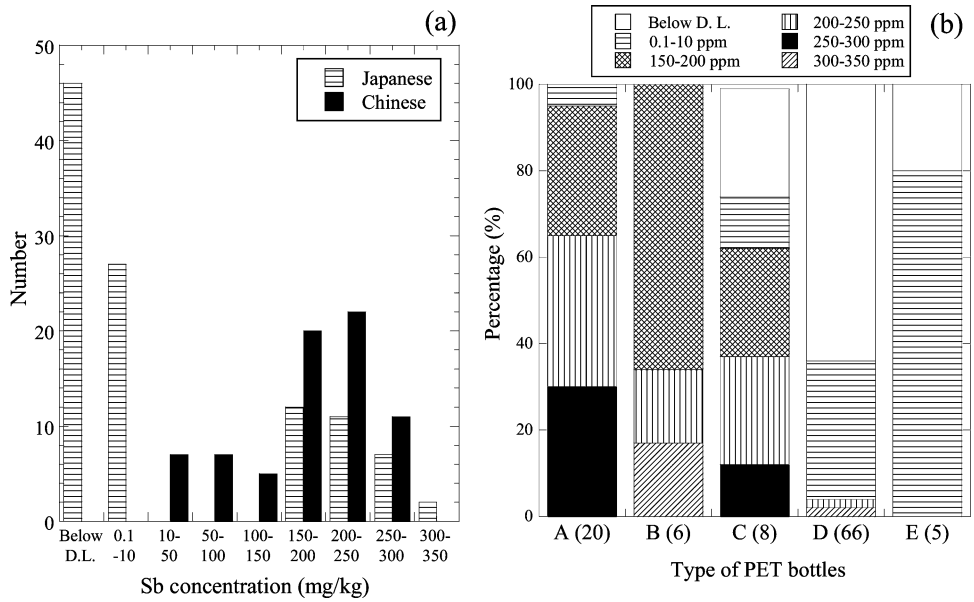

FIGURE 1. (a) Concentrations of Sb in PET bottles sold in Japan and China. (b) Concentrations of Sb in PET bottles in Japan for various use. (A): bottles for aseptic cold filling normally used for noncarbonated cold drinks; (B): pressure tight bottles for carbonated drinks; (C): heat resistant and pressure tight bottles for semisparkling drinks; (D): heat resistant bottles for hot filling such as for hot teas; (E): bottles for freezer. Numbers in parentheses indicate the number of sample for each type. D.L. means detection limit.

in the solution after the decomposition in most cases. Thus, other methods using various types of acids coupled with microwave digestion or heating using a hot plate were utilized to decompose PET. Finally, we found that 98% H_2SO_4 was the best way to decompose PET. A precisely weighed PET (50 mg) initially rinsed with pure water (Milli-Q water, Millipore; conductivity: 18.3 MΩ) before the decomposition process was soaked in 2 mL of 98% H_2SO_4 in PTFE digestion vessels. In most cases, PET digests completely after 4 h in 98% H_2SO_4 without heating or microwave treatment. To ensure complete digestion, the PTFE digestion vessels with lids were heated up to 280 °C on a hot plate for 12 h, in which it was confirmed that no Sb was lost during the heating processes. The digested solution was diluted to a 50 mL mixture with 2% HNO_3 and In (concentration: 10 ng/g) was added to the solution as an internal standard for the measurement by ICP-MS (Agilent 7500 CS). The influence of sulfate ion in the decomposed solution was also examined. It was shown that the presence of sulfate ion at the concentration level (<4 wt %) used for the measurements did not change the Sb signal in the ICP-MS detection. Repeated analysis of one PET sample ($N = 5$) showed that the precision (1σ) of our analyses was 3.5%. In addition, Sb concentrations were measured for PET samples taken from three parts (upper, middle, and lower) of one PET bottle. The 1σ of the Sb concentrations was 2.6%, showing that there were no appreciable differences in Sb concentrations in PET resin taken from the different portions of one PET bottle. Standard materials of PET containing Sb were not available, so the Sb concentrations in standard soil (JSO-1; Sb 0.38 μg/g) and rock (JG-1; Sb 0.13 μg/g) samples received from the Geological Survey of Japan (*16*, *17*) were repeatedly measured with acid decomposition using $HF/HClO_4$. The Sb concentrations measured were within ±11% of the recommended values.

2.3. XAFS Analysis. About 10 pieces of PET bottles cut into 2 cm squares were piled and packed in an Sb-free polyethylene bag to be exposed to an incident X-ray for XAFS measurement in fluorescence mode. Antimony K-edge XAFS spectra were measured at room temperature under ambient air conditions at the beamline BL01B1 in SPring-8 (Hyogo, Japan) as described in Mitsunobu et al. (*11*). The EXAFS data were analyzed by REX2000 (Rigaku Co. Ltd.) as reported previously (*11*). Fourier transformation of the $k^2\chi(k)$ EXAFS oscillation from k space to r space was performed with a range of 3.0−11.0 Å^{-1} to obtain a radial distribution function (RSF) for Sb. Inversely, Fourier filtered data were analyzed through the usual curve fitting method. Theoretical phase shifts and amplitude functions employed in this fitting procedure were calculated by FEFF 7.0 (*18*). The phase shifts and amplitude functions of Sb−O and Sb−Sb were extracted from the structure of Sb_2O_3 (*19*), whereas those for Sb−C were from that of dihydroxytrimethylstiborane carbonate hydrate (*20*). The uncertainty in the analysis can be estimated from the Res factor given by the equation as Res (%) = $(\sum\{k^2\chi_{obs}(k) - k^2\chi_{cal}(k)\}^2)/(\sum\{k^2\chi_{obs}(k)\}^2)$, where $\chi(k)_{obs}$ and $\chi(k)_{cal}$ are the experimental and theoretical data points, respectively.

2.4. Leaching Experiments. Exactly 0.100 g each of five PET bottle samples cut into 2 × 2 mm^2 pieces rinsed with Milli-Q water was soaked in a 2.0 g of Milli-Q water in PTFE vessel at 40 °C in a water bath. After 30 or 45 days, Sb concentration in the water was measured by ICP-MS as described above. The sample for the measurement was acidified to 2% HNO_3 before the ICP-MS analyses. The blank test was done for Sb in Milli-Q water similarly treated without adding the PET pieces, showing that the contribution of the blank was less than 2% of the Sb that leached into the water from the PET samples. For the three PET samples, similar experiments were done using other solvents such as 4 wt% acetic acid, ethanol (20 wt% in water), and humic acid solution (20 mg/L; humic acid sample was extracted from paddy soil, ref (*21*)). Acetic acid and ethanol were also employed in Nishioka et al. (*5*).

3. Results and Discussion

3.1. Sb Concentrations in PET Bottles. Antimony concentrations were determined for all the Chinese ($N = 72$) and Japanese ($N = 105$) samples collected in this study. Concentration of Sb in some PET bottles reached up to about 300 mg/kg (Figure 1a). The proportion of PET bottles with Sb more than 10 mg/kg was 30.5% in Japan and 100% in China. According to the χ^2 test, a hypothesis that the distributions are different between Chinese and Japanese PET bottles was valid with a probability above 0.995. Nishioka

et al. (*5*) reported the Sb concentrations in seven Japanese bottles, wherein the Sb concentrations ranged from 168 to 216 mg/kg, which are basically consistent with the results obtained here. Generally, PET bottles can be classified into five to six species depending on their use: (A) bottles for aseptic cold filling mainly used for noncarbonated cold drinks; (B) pressure-tight bottles for carbonated drinks; (C) heat-resistant and pressure-tight bottles for semisparkling drinks; (D) heat-resistant bottles for hot filling like hot teas; and (E) bottles for freezing. When the results were confined to Japanese PET bottles, it was found that most of the PET bottles categorized into types A and B contained Sb at more than 150 mg/kg (Figure 1b). In addition, about half of the type C bottles also contained large amounts of Sb. The independence of the Sb concentration and the type of PET bottles was also tested by the χ^2 test. The *p*-value was 0.002, which shows that the Sb concentration depends on the type of PET bottle. All the Chinese PET bottles belonged to types of A, B, and C, which might be related to the larger rate of Sb-contained PET bottles in China. With regard to other parameters such as thickness and manufacturer of the beverages (Figure S1 in the Supporting Information), *p*-values in the χ^2 test for independence were 0.79 and 0.99, respectively, showing that these parameters are independent of the Sb concentration in the PET bottles.

3.2. XANES Analysis. To obtain the information on the oxidation states of Sb in the PET samples, XANES at the Sb K-edge was obtained for 12 PET samples, which were named samples A to L. The details of the bottles such as the type of use and Sb concentration are given in Table S1 in the Supporting Information. Due to the detection limit of XANES, the samples with Sb concentrations above 150 mg/kg for all types of the beverages were chosen for the XANES analyses (Figure 2). The oxidation state of Sb can be estimated based on the shift of the XANES peak (*8, 11*), as seen from the spectra of $Sb(OH)_6^-$ and Sb_2O_3. Among the samples, sample A had a peak at the position identical to that of Sb_2O_3, suggesting that Sb(III) was the oxidation state of Sb in sample A. From samples B to L, the peak gradually shifted to higher energy, implying that Sb(V) was also incorporated in the PET samples. The Sb(V)/Sb(III) ratio was determined by simulating the spectra through the linear combination of the spectra of Sb_2O_3 and $Sb(OH)_6^-$ based on least-squares analysis in the energy range between 30.452 and 30.513 keV (Figure 2). As Sb(V) reference, Sb_2O_5 and $Sb(OH)_6^-$ were tested. Consequently, $Sb(OH)_6^-$ was selected because the difference between the spectra of most of the samples and simulated curves were smaller when using $Sb(OH)_6^-$ as the Sb(V) reference. As a result, it was estimated that sample L had the highest Sb(V)/Sb(III) ratio (Sb(V) fraction: 51%), whereas the Sb(III) fractions of the other samples were estimated to be between 61 and 99% (Table S1 in the Supporting Information). The precision of this method was estimated to be 6.4% as the absolute value to the Sb(III) or Sb(V) fraction (%) data (Figure S2 in the Supporting Information). The Sb fraction data can be relatively changed to some degree by the selection of Sb(V) reference sample for the simulation since the spectra of Sb_2O_5 and $Sb(OH)_6^-$ are different (*8*). However, the order of the sample in terms of the Sb(V)/Sb(III) ratio may not be affected by the selection since the energy of the XANES peak actually shifted to higher energy as the Sb(V) fraction value increases.

The Sb(V)/Sb(III) was not correlated with Sb content in the PET bottles (r^2 = 0137; *r*: correlation coefficient) as indicated in Figure S3 in the Supporting Information. The variation of the Sb(V)/Sb(III) ratio was also compared with the type of PET bottle (type A to E) as discussed in the previous section. However, any correlation between them was not found either. There was apparently no concrete explanation for the variation of the Sb(V)/Sb(III) ratios in the PET samples.

3.3. EXAFS Analysis. EXAFS in *k* space (Figure 3a) for

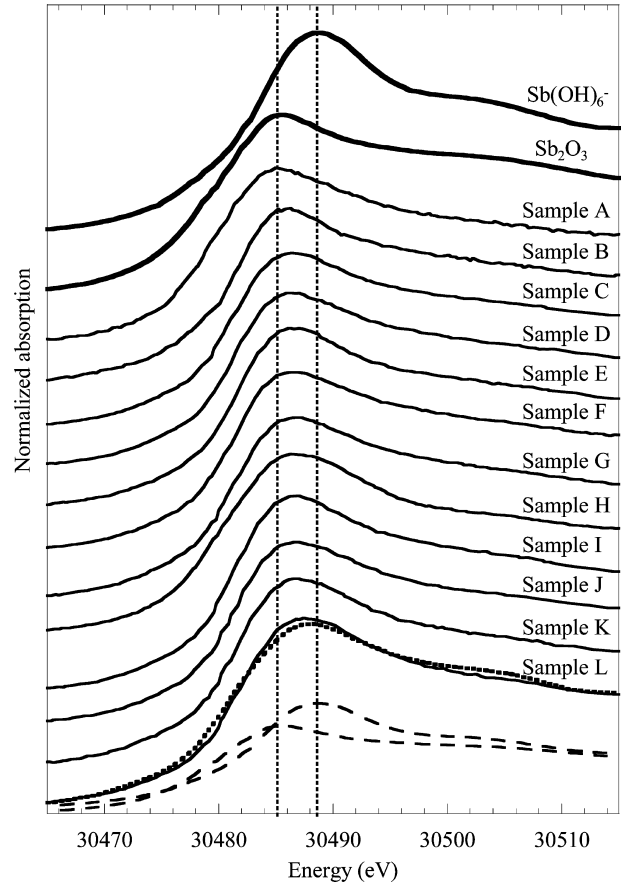

FIGURE 2. XANES spectra at Sb K-edge for Sb in various PET samples (A–L) with those for Sb_2O_3 and $Sb(OH)_6^-$. Presence of both Sb(III) and Sb(V) at various Sb(III)/Sb(V) ratios is suggested. Simulation result was shown for Sample L with the contributions of Sb(III) and Sb(V) species indicated by broken curves.

samples A and F with XANES peaks at slightly different energies (approximately 2 eV), or with different Sb(III) fractions (99% and 68%, respectively), showed EXAFS oscillations similar to those of Sb_2O_3, $Sb(OH)_6^-$, and Sb_2O_5 in *k* space (Figure 3a). In a radial structural function (RSF) in *R* space (Figure 3b; phase shift uncorrected), Sb_2O_3, $Sb(OH)_6^-$ ion, and Sb_2O_5 had peaks around $R + \Delta R = 1.5$ Å corresponding to oxygen as a first neighboring atom.

The results for the reference materials studied here are briefly given hereinafter. More details of Sb EXAFS for other Sb inorganic compounds were thoroughly studied in Scheinost et al. (*8*). Based on the structures of Sb_2O_3 reported in Svensson (*19*), three oxygens are placed around Sb as a first neighboring atom (Sb—O_1 shell) at the Sb—O interatomic distance of 1.971 Å in Sb_2O_3. The second and third neighboring atoms were oxygen (Sb—O_2 shell; coordination number (CN) = 3) and Sb (Sb—Sb_1 shell; CN = 3) at a distance of 2.917 and 3.618 Å, respectively. The EXAFS simulation of the first peak for Sb_2O_3 based on the Sb—O parameters generated by FEFF gave an Sb—O_1 length of R_{Sb-O_1} = 1.971 Å with CN = 3.0, which is identical to the values in the literature. Although the second neighboring atom was also oxygen (Sb—O_2), its contribution to EXAFS oscillation in *k* space was smaller than that of Sb—Sb as the third neighboring atom (Sb—Sb_1 shell) except for a smaller *k* region ($k < 6$ Å^{-1}; Figure 3a). Optimized parameters were R_{Sb-O_2} = 2.876 Å and CN = 2.0 for Sb—O_2 shell, while R_{Sb-Sb_1} = 3.626 Å and CN = 2.5 were obtained for the Sb—Sb_1 shell. These parameters could also be accepted considering the precisions shown in Table 1 and the accuracies (*R*: ± 0.02 Å; CN: ± 20%; σ^2: ± 20%) of the EXAFS

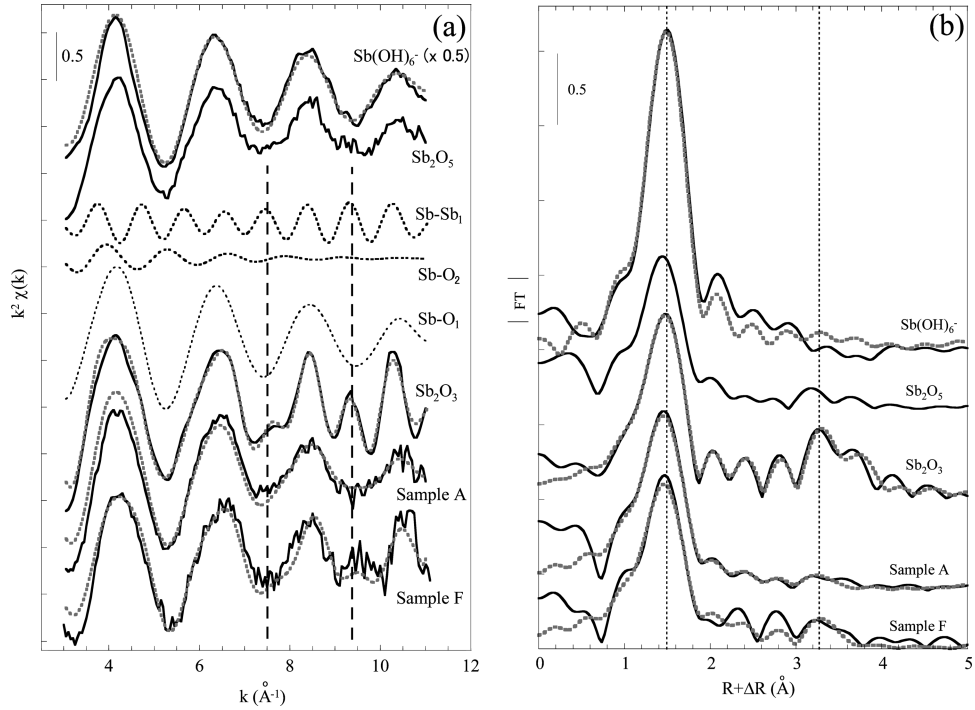

FIGURE 3. EXAFS spectra at Sb K-edge for Sb in PET samples (A and F) in *k* space (a) and *R* space (b). Gray curves indicate the simulation results. Contributions of Sb—O_1, Sb—O_2, and Sb—Sb_1 in the spectrum of Sb_2O_3 in *k* space were also indicated.

TABLE 1. Exafs Parameters Obtained by the Simulation Using Parameters Generated by FEFF 7.02 (*18*)[a]

sample	shell	CN	*R* (Å)	ΔE_0 (eV)	σ^2 ($\times 10^3$)	res (%)
sample A (3.0 < *k* < 11.0)	Sb—O_1	3.4 ± 0.6	1.969 ± 0.016	5.7 ± 2.0	5.2 ± 1.8	0.49
	Sb—O_2	0.8 ± 0.2	2.879 ± 0.170		11.9[b]	
	Sb—Sb_1	0.4 ± 0.1	3.571 ± 0.097		3.0[b]	
sample F (3.0 < *k* < 11.0)	Sb—O_1	3.2 ± 0.6	1.961 ± 0.016	6.9 ± 2.0	4.9 ± 1.8	3.0
	Sb—O_2	1.4 ± 0.1	2.847 ± 0.170		11.9[b]	
	Sb—Sb_1	0.9 ± 0.1	3.576 ± 0.001		3.0[b]	
Sb_2O_3(3.0 < *k* < 11.0)	Sb—O_1	3.0 ± 0.6	1.971 ± 0.016	4.7 ± 2.2	2.7 ± 0.3	0.84
	Sb—O_2	2.0 ± 0.1	2.876 ± 0.074		11.9 ± 0.3	
	Sb—Sb_1	2.5 ± 0.1	3.626 ± 0.035		3.0 ± 0.1	
	Sb—Sb_2	2.3 ± 0.9	3.938 ± 0.050		3.0*	
$Sb(OH)_6^-$(3.0 < *k* < 11.0)	Sb—O_1	5.5 ± 0.9	1.974 ± 0.014	3.6 ± 2.4	1.4 ± 1.3	0.44

[a] CN: coordination number; *R*: interatomic distance; ΔE_0: threshold E_0 shift; σ: Debye-Waller term. Least squares precisions are given to each value. [b] Errors in the fitted parameters were estimated to be generally ± 0.02 Å for *R*, ± 20% for N, and 20% for σ^2 (*22*).

analyses (*22*). On the other hand, the structure of $Sb(OH)_6^-$ ion in $NaSb(OH)_6$ (*23*) showed that the distance between Sb and O was in the range of 1.972−1.999 Å in which the average value was 1.983 Å. The EXAFS parameters obtained for the $Sb(OH)_6^-$ ion such as R_{Sb-O} = 1.974 Å and CN = 5.5 were also acceptable as compared with the literature data (*23*). These results show that the EXAFS analyses in our study are reliable for the determination of the Sb local structure in PET bottles.

The R_{Sb-O_1} for sample A determined by EXAFS was R_{Sb-O_1} = 1.969 Å, which was similar to that of either Sb_2O_3 or $Sb(OH)_6^-$. A similar value was also obtained for sample F (R_{Sb-O_1} = 1.961 Å), and these results showed that the atom binding to Sb in the PET bottles was most likely to be oxygen. Based on the chemical composition of PET, an Sb—C bond is also possible due to the presence of C as the major component of PET. Thus, the first peak was simulated by the Sb—C parameters obtained by FEFF based on the structure of methyl-Sb species in $(CH_3)_3Sb(OH)_2CO_3$ (*20*). The interatomic distances of Sb—C determined based on the assumptions were R_{Sb-C} = 2.025 Å and 2.016 Å for samples A and F, respectively. In fact, the distances were significantly shorter than those of the Sb—C reported for various alkyl Sb species ranging from 2.09 to 2.15 Å (e.g., (*25*−*27*),). Hence, the results strongly suggest that C is not the main Sb neighboring atom in the PET samples.

Since Sb_2O_3 is the starting material added as a catalyst for the production of PET, it is possible that a part of Sb_2O_3 remained in the PET bottles. To find out the presence of Sb_2O_3, EXAFS parameters assuming the presence of Sb—Sb_1 shell for the samples were compared with those of Sb_2O_3. During the simulation, the Debye−Waller factors for Sb—O_2 and Sb—Sb_1 shells were fixed identically to those obtained for Sb_2O_3 for samples A and F. The Sb—Sb_2 shell was not included in the samples because there was no improvement in the fitting of the spectra by considering the Sb—Sb_2 shell. As shown in the RSFs of Sb_2O_3, a peak due to the Sb—Sb_1 pair was observed in the RSF at $R + \Delta R$ = 3.25 Å (phase shift uncorrected). The simulation of the peak gave structural parameters such as R_{Sb-Sb_1} = 3.626 Å and CN = 2.5 (±0.1) for Sb_2O_3. For sample A, the peak at $R + \Delta R$ = 3.25 Å in the RSF was smaller than that of Sb_2O_3. The imaginary part of the FT also had a symmetric peak at the position close to that in the FT magnitude (Figure 4S in the Supporting Information), suggesting that the assignment of Sb—Sb_1 shell at $R + \Delta R$ =

3.25 Å was reasonable (*12*). Assuming a peak in the position, the simulation suggested that the interatomic distance of Sb—Sb_1 and the CN value for the RSF peak at $R + \Delta R = 3.25$ Å were 3.571 Å and 0.4 (±0.1), respectively, for sample A. The CN value showed that the contribution of Sb—Sb_1 scattering was not very important for Sb EXAFS in the PET compared with that in Sb_2O_3. If the Sb atom was surrounded by PET polymers consisting of light elements (C, H, and O), the contribution of the scattering of these light elements in the EXAFS may not be strong compared with the neighboring Sb atom present close to the center Sb atom. Hence, the CN value of Sb—Sb_1 in the PET bottle normalized by that of Sb_2O_3 roughly shows the fraction of Sb_2O_3 among the total Sb species in PET. Based on the assumption, the Sb as Sb_2O_3 in sample A was estimated to be 16% (= 0.4/2.5), showing that Sb_2O_3 is a minor Sb species in PET.

For sample F, the peak at $R + \Delta R = 3.25$ Å (phase shift uncorrected) in the RSF was somewhat clearer. In k space, the presence of the Sb—Sb_1 shell for Sb_2O_3 induced peaks or shoulders at $k = 7.6$ and 9.4 $Å^{-1}$ as seen in the contribution of the Sb—Sb_1 shell (Figure 3a). The EXAFS simulation showed that the CN for Sb—Sb_1 in sample F was 0.9 (±0.1), suggesting that the Sb_2O_3 fraction was at most 36% in the sample. This still shows that Sb_2O_3 is not the main Sb species in the PET bottle.

The EXAFS spectra at k spaces for samples A and F were also simulated by a model represented as $\alpha \times (1 - \beta) \times$ (Sb—O) $+ \beta \times$ (Sb_2O_3) in the k range from 3.5 to 11 $Å^{-1}$, where (Sb—O) represents a single Sb—O path and (Sb_2O_3) represents the whole set of Sb—O and Sb—Sb paths optimized for Sb_2O_3. In this simulation, the CN for the non-Sb_2O_3 Sb—O is α and the fraction of Sb in the form of Sb_2O_3 is β. As a result, α values were 2.7 and 2.5 for the samples A and F, respectively. The β values were 15 and 17% for the two samples, respectively, confirming that Sb_2O_3 is not a predominant Sb species in the PET bottles.

The discussion here assumes that Sb_2O_3 in PET, if present, is ordered as the bulk Sb_2O_3. If Sb_2O_3 in PET bottles forms nanoparticles, the contribution of Sb—O can be lower in the EXAFS spectra as found for Cu nanoparticles in soil (*28*). Small Sb_2O_3 particles at the micrometer scale were not found by the synchrotron-based micro-XRF at BL37XU in SPring-8 (beam size: $1.3 \times 0.9\ \mu m^2$), but the method cannot be applied to nanoparticles. The presence of nanoparticles of Sb_2O_3 must be surveyed by transmission electron microscopy (TEM) in the future.

The results of Sb species suggested by XAFS were compared with the production processes of PET with Sb in the polycondensation reactions. During solid-state polycondensation (SSP) with the addition of Sb, it was suggested that Sb_2O_3 added to the prepolymers was not incorporated into the polycondensation reactions (*1*). It was also suggested that the incorporated Sb existed as either Sb glycolate only or Sb glycolate binding to the end group of the PET polymer, whereas other Sb added as Sb_2O_3 is generally excluded from the polymers. From this reaction scheme, the neighboring atom of Sb should be oxygen. In addition, the number of oxygen coordinated to Sb is estimated to be three based on the reaction processes (*1*). The CN value of oxygen (Sb—O_1) obtained by the EXAFS for sample A (= 3.4) was close to three, which is also consistent with the polycondensation reactions (*1*).

According to the XANES data, Sb in the samples was partially oxidized to Sb(V) which could have a larger CN value considering the structures of Sb(V) in Sb_2O_5 (*24*) and $Sb(OH)_6^-$, where Sb is surrounded by six oxygen atoms. However, the CN value of sample F which contained an Sb(V) fraction of 32% based on the XANES analysis was 3.2, similar to those of sample A and Sb_2O_3. The reason for the results is not clear at present, but the Debye—Waller factor (σ^2) of Sb—O_1 in sample F was larger than that of Sb_2O_3, suggesting that the distances from the center Sb to three oxygens in the PET bottle were disordered to a larger degree than that of Sb_2O_3. Although such disorder is suggested to some degree, the CN value close to 3 shows that the coordination environment of Sb was not seriously affected by the oxidation of Sb(III) within the PET bottle. The results should be considered important when evaluating the leaching behavior of Sb in water.

TABLE 2. Concentrations of Sb Leached from PET Resin (0.10 g) to Milli-Q Water (2.0 g) after 30 and 45 Days for Samples A, C, F, K, and L

sample	Sb in PET (mg/kg)	Sb(III) fraction (%)[a]	elapsed time (days)	Sb in water (μg/kg)[b]	leached fraction[c] ($\times 10^5$)
A	275	99	30	0.874 ± 0.039	6.36 ± 0.28
C	260	73	30	2.75 ± 0.08	21.2 ± 0.62
			45	2.41 ± 0.08	18.5 ± 0.62
F	257	68	30	4.44 ± 0.01	34.3 ± 0.1
			45	2.42 ± 0.03	18.7 ± 0.2
K	154	61	30	1.34 ± 0.01	17.4 ± 0.1
			45	1.33 ± 0.01	17.3 ± 0.1
L	260	49	30	0.851 ± 0.153	6.55 ± 1.18
			45	2.43 ± 0.08	18.7 ± 0.6

[a] Error of the value is estimated to be ± 6.4% (Figure S2 in the Supporting Information). [b] Error indicated is 1σ of repeated analyses (N = 3). [c] Sb concentration leached in water was normalized by Sb concentration in PET.

3.4. Leaching Behavior. It is possible that the leaching behavior of Sb can be due to the oxidation state and local structure of Sb in PET, as suggested in other environmental studies (*8*–*11*). Hence, the leaching behavior of Sb into water was examined for five PET samples (samples A, C, F, K, and L) by soaking them in Milli-Q water at 40 °C for 30 and 45 days. The final pH was not very low (3.5 < pH < 4.5), so it is possible that Sb(III) with low solubility can precipitate even if it leached into water once. However, Sb amount dissolved by acid treatment was negligible (less than 5% of the amount of Sb that leached to water), showing that the presence of Sb precipitates could be discounted in the leaching experiments.

The results shown in Table 2 indicate that the Sb concentration that leached in water ranged from 0.874 to 4.40 μg/kg. When normalized by the original Sb amount in each PET sample, the Sb fraction that leached into water accounted for less than 0.034% of the total Sb initially contained in the PET samples. The allowable limit of Sb concentration in drinking water is 2.0 μg/kg in Japan (*5*); the Sb concentrations in Table 2 are comparable to this limit and should be taken seriously. However, this discussion is not extended here, because the aim of this study is to reveal the speciation of Sb in PET and to find any possible relationships between Sb species and the Sb fraction that leached in water. Although Sb(V) may be more soluble than Sb(III) as seen in the solubility diagrams calculated by MINTEQ (Figure S5 in the Supporting Information), the concentration of Sb that leached from PET (Table 2 and Figure S3 in the Supporting Information) does not depend on the Sb(V) fraction in the PET ($r^2 = 0.018$). This is not a surprising result because Sb is not incorporated to PET as an inorganic species but mainly as an organo—metal complex with PET as shown by the EXAFS data. However, as indicated in the previous section, the low CN value of the first neighboring oxygen (Sb—O_1) in sample F indicates that Sb is oxidized without changing the local structure of Sb(III) initially incorporated into the PET polymers. These results suggest that the degradation of PET itself is primarily an important factor that governs the Sb leaching into water. For samples

C, F, and K, leaching behavior of Sb was also examined for other solvents such as 4% acetic acid (pH 2.3), ethanol (20% in water), and humic acid solution (20 mg/L, pH 4). As a result, the leached fraction of Sb decreased in the order of sample F > Sample C ≈ sample K for all the four solvents including water (Figure S6 in the Supporting Information). The results suggest that the leaching behavior of Sb depends on the nature of each PET bottle, which is consistent with our suggestion that Sb leaching is controlled by the degradation of the PET bottle itself. The results implied that PET of sample F can be readily subject to degradation to a larger degree than the other bottles.

This conclusion is supported by Westerhoff et al. (*6*) who showed the effects of pH, temperature, and sunlight on Sb leaching. First, the acidification did not increase the Sb concentration in their study. If the Sb release is a function of inorganic Sb(III) fraction that can be less soluble at higher pH, then Sb leaching can be a function of pH, which is not the case for Sb leaching in PET (*6*). On the other hand, higher temperature and sunlight caused the release of Sb to a larger degree. It is most likely that the temperature and sunlight can facilitate the degradation of PET itself. Based on the information coupled with the speciation of Sb in PET in this study, the degradation of PET itself is more important for the Sb leaching rather than Sb speciation in PET bottles.

Acknowledgments

We are grateful to Prof. K. Sugimori (Toho University) for providing some PET bottle samples. This study was funded by funds from the Ministries of Education, Culture, Sports, Science, and Technology and Environment of Japan. G.Z. acknowledges financial support as 100-Tallent program from CAS. This work has been performed with the approval of SPring-8 (No. 2007A2065, 2007B1175, and 2007B1332).

Supporting Information Available

Details of XANES and EXAFS results, Sb contents in PET, and leaching behavior of Sb into various solvents. This material is available free of charge via the Internet at http://pubs.acs.org.

Literature Cited

(1) Duh, B. Effect of antimony catalyst on solid-state polycondensation of poly(ethylene terephthalate). *Polymer* **2002**, *43*, 3147–3154.

(2) Thiele, U. K. Quo vadis polyester catalyst. *Chem. Fibers Int.* **2004**, *54*, 162–163.

(3) Shotyk, W.; Krachler, M.; Chen, B. Contamination of Canadian and European bottled waters with antimony leaching from PET containers. *J. Environ. Monit.* **2006**, *8*, 288–292.

(4) Shotyk, W.; Krachler, M. Contamination of bottled waters with antimony leaching from polyethylene terephthalate (PET) increases upon storage. *Environ. Sci. Technol.* **2007**, *41*, 1560–1563.

(5) Nishioka, K.; Hirahara, A.; Iwamoto, E. Determination of antimony in polyethylene terephthalate bottles by graphite furnace atomic absorption spectrometry jsing microwave sample preparation. *Bull. Inst. Life Sci. Hiroshima Prefectural Womens's Univ.* **2002**, *8*, 35–42.

(6) Westerhoff, P.; Prapaipong, P.; Shock, E.; Hillaireau, A. Antimony leaching from polyethylene terephthalate (PET) plastic used for bottled drinking water. *Water Res.* **2008**, *42*, 551–556.

(7) Hansen, H. R.; Pergantis, S. A. Detection of antimony species in citrus juices and drinking water stored in PET containers. *J. Anal. Atomic Spectrom.* **2006**, *21*, 731–733.

(8) Scheinost, A. C.; Rossberg, A.; Vantelon, D.; Xifra, I.; Kretzschmar, R.; Leuz, A. K.; Funke, H.; Johnson, C. A. Quantitative antimony speciation in shooting-range soils by EXAFS spectroscopy. *Geochim. Cosmochim. Acta* 200670, 3299–3312.

(9) Filella, M.; Belzile, N.; Chen, Y.-W. Antimony in the environment: a review focused on natural waters. II. Relevalent solution chemistry. *Earth-Sci. Rev* **2002**, *57*, 125–176.

(10) Filella, M.; Belzile, N.; Chen, Y.-W. Antimony in the environment: a review focused on natural waters I. Occurrence. *Earth-Sci. Rev* **2002**, *59*, 265–285.

(11) Mitsunobu, S.; Harada, T.; Takahashi, Y. Comparison of antimony behavior with that of arsenic under various soil redox conditions. *Environ. Sci. Technol.* **2006**, *40*, 7270–7276.

(12) Teo, B. K. *EXAFS: Basic Principles and Data Analysis*; Springer-Verlag: New York, 1986.

(13) Brown, G.E. Jr.; Sturchio, N. C. An overview of synchrotron radiation applications to low temperature geochemistry and environmental science. *Rev. Mineral. Geochem.* **2002**, *49*, 1–115.

(14) Takahashi, Y.; Minamikawa, R.; Hattori, H. K.; Kurishima, K.; Kihou, N.; Yuita, K. Arsenic behavior in paddy fields during the cycle of flooded and non-flooded periods. *Environ. Sci. Technol.* **2004**, *38*, 1038–1044.

(15) Takahashi, Y.; Kanai, Y.; Kamioka, H.; Ohta, A.; Maruyama, H.; Song, Z.; Shimizu, H. Speciation of sulfate in size-fractionated aerosol particles using sulfur K-edge X-ray absorption near-edge structure (XANES). *Environ. Sci. Technol.* **2006**, *40*, 5052–5057.

(16) Imai, N.; Terashima, S.; Itoh, S.; Ando, A. 1994 compilation values for GSJ reference samples, "Igneous rock series". *Geochem. J.* **1995**, *29*, 91–95.

(17) Terashima, S.; Imai, N.; Taniguhci, M.; Okai, T.; Nishimura, A. Preparation and preliminary characterisation of four new GSJ geochemical reference materials: soils, JSO-1 and JSO-2 soil; and marine sediments, JMS-1 and JMS-2. *Geostand Newslett.* **2002**, *26*, 85–94.

(18) Zabinsky, S. I.; Rehr, J. J.; Ankudinov, A.; Albers, R. C.; Eller, M. J. Multiple-scattering calculations of X-ray-absorption spectra. *Phys. Rev. B* **1995**, *52*, 2995–3009.

(19) Svensson, C. Refinement of the crystal structure of cubic antiomony trioxide, Sb_2O_3. *Acta Crystallogr., B* **1975**, *31*, 2016–2018.

(20) Lang, G.; Klinkhammer, K. W.; Recker, C.; Schmidt, A. Dihydroxytrimethylstiboran—Einige Eigenschaften und Struktur. *Z. Anorg. Allg. Chem.* **1998**, *624*, 689–693.

(21) Takahashi, Y; Minai, Y; Ambe, S; Makide, Y; Ambe, F. Comparison of adsorption behavior of multiple inorganic ions on kaolinite and silica in the presence of humic acid using the multitracer technique. *Geochim. Cosmochim. Acta* **1999**, *63*, 815–836.

(22) O'Day, P. A.; Rehr, J. J.; Zabinsky, S. I.; Brown, G. E. Extended X-ray absorption fine structure (EXAFS) analysis of disorder and multiple scattering in complex crystalline solids. *J. Am. Chem. Soc.* **1994**, *116*, 2938–2949.

(23) Asai, T. Refinement of the crystal structure of sodium hexahydroxoantimonate(V), $NaSb(OH)_6$. *Bull. Chem. Soc. Jpn.* **1975**, *48*, 2677–2679.

(24) Jansen, M. Die Kristallstruktur von Antimon(V)-oxid. *Acta Crystallogr., Sect. B: Struct. Sci.* **1979**, *35*, 539–542.

(25) Behrens, U.; Breunig, H. J.; Denker, M.; Ebert, K. H. Iodketten in $(Me_4Sb)_3I_8$ und isolierte Triiodide-Ionen in Me_4AsI_3. *Angew. Chem.* **1994**, *106*, 1023–1024.

(26) Britton, D.; Young, V.G.Jr.; Schlemper, E. O. Intermolecular interactions in cyanodimethylarsine and cyanodimethylstibine. *Acta Crystallogr., Sect. C: Cryst. Struct. Commun.* **2002**, *58*, m307–m309.

(27) Breunig, H. J.; Lork, E.; Rösler, R.; Becker, G.; Mundt, O.; Schwarz, W. Common features in the crystal structures of the compounds bis(dimethylstibanyl)oxane and sulfane, and the minerals valentinite and stibnite (Grauspiessglanz). *Z. Anorg. Allg. Chem.* **2000**, *626*, 1595–1607.

(28) Manceau, A.; Nagy, K. L.; Marcus, M. A.; Lanson, M.; Geoffroy, N.; Jacquet, T.; Kirpichtchikova, T. Formation of metallic copper manoparticles at the soil-root interface. *Environ. Sci. Technol.* **2008**, *42*, 1766–1772.

ES802073X